Journal of Radioanalytical and Nuclear Chemistry (2018) 315:1–12
https://doi.org/10.1007/s10967-017-5641-z

Determination of lead isotope ratios in uranium mine products in South Africa by means of inductively coupled plasma mass spectrometry

Manny Mathuthu[1] · Ntokozo Khumalo[1]

Received: 17 December 2016 / Published online: 2 December 2017

Abstract
Nuclear terrorism has led to newer investigative methods for building national nuclear forensic libraries. The objective of this work was to resolve these signatures by applying the ICP-MS for isotope ratio (IR) analysis on uranium containing samples. Lead (Pb) isotope ratios for the studied gold mine has $^{207}Pb/^{204}Pb$ values between 13–20 and $^{206}Pb/^{204}Pb$ values ranging from 16–25, which confirm that the Carletonville gold fields are of uraninite detrital pyrite deposits. Trace elemental concentrations indicated a pyrite type of uranium deposit. Uranium in the deposit exhibits geochemical signatures of the radiogenic formations of the ore enhanced in ^{206}Pb.

Keywords Mining products · Uranium · ICP-MS · Lead isotopic ratio · Nuclear forensic signatures

Introduction

The construction of nuclear reactors as a source of reliable green energy has gained momentum in many countries of the world in recent years. However there are rising nuclear security concerns about the safety and proliferation of the nuclear materials used in these nuclear power plants [1–3] as well as possible diversion for illicit purposes by nuclear terrorists [4, 5]. This has necessitated the characterization of seized nuclear or radioactive material based on chemical and isotopic composition as well as physical parameters which can be used in determining the origin of the interdicted radiological nuclear material. The characteristic difference between lead isotopic composition from the earth's crust (e.g. uranium ore body) and that from industrial emissions enables the applications of this ratio in nuclear forensics investigations [6].

In South Africa there is a vast uranium ore (uraninite) deposits [7], with a lot of mining and processing activities. It is therefore imperative for each the country to properly collect and compile nuclear forensic signatures in databases and national libraries, that can be used as evidence for attribution of the seized nuclear or radioactive material.

Many instruments are being used to apply various analytical techniques for chronometric analysis of intercepted nuclear materials from a nuclear facility. The LA ICP-MS or laser-ablation micro-sampling (LAM-ICP-MS) are some of the Instruments that have been used for determining the lead isotopic signatures of the material at the front or back end of the nuclear fuel cycle [8–10]. Recent study by Fuchs et al., used a LA-ICP-MS to measure trace elements (provenance of uranium) on the samples taken from the Transvaal Supergroup (which included the Carletonville Gold field) in South Africa, and their results showed that the higher U and gold concentrations are embedded in the pyrite rock [7].

The objective of this work was to demonstrate the use of the Perkin Elmer 300Q ICP-MS as a viable tool for resolving nuclear forensic signatures from a uranium mine in South Africa. Results from the first stage in the fuel cycle are described here, and the data presented could form a basis for a South African nuclear forensics library. However, a comprehensive nuclear forensic library can only be developed when all the stages in the fuel cycle have been investigated. This work describes the investigation of Pb isotopic composition and trace elemental

✉ Manny Mathuthu
Manny.Mathuthu@nwu.ac.za

[1] Center for Applied Radiation Science and Technology (CARST), North-West University (Mafikeng), Mmabatho 2735, South Africa

analysis to determine respectively the fingerprint lead signatures and the provenance of the uranium in the uraninite ore. Interpretation of the results for possible tracing (attribution) of the origins of South African Pb is presented. We also discus limitations of Pb isotopic fingerprinting technique in this work [11].

Materials and methods

Study area

The study area is indicated in Fig. 1 and the authors cannot give further details due to confidentiality agreements.

Geaology of the mining site

The sampling site falls within the Carletonville goldfields which is part of the so called B-Reef or Witwatersrand Supergroup) of South Africa. The uraninite (UO_{2x}) [12] deposits here are unconformity in nature lying on the sedimentary succession of the Witwatersrand Supergroup, with an estimated age of about 2.59 Ga [7]. Gold (and uranium) mining uses the underground mining techniques as the mines are each estimated to be more than 2 km deep. These mines are now over 132 years old, [13] and are still operational.

Sample collection

The Carletonville goldfields have a quartz-pebble conglomerate, intercalated with chert, jasper pebbles and minor shales, bound within siliceous to slightly argillaceous rocks, and in this work, we sampled from mining operations in the Carletonville gold fields [7].

The tailing dams in Fig. 1 are located on the RHS of DSW7/12 (T3 no separate Fig.); below DSW43/19 (T3 no separate Fig.), between DSW40/7 & DSW18/3 (T1 in Fig. 2) and above WV15 (T2 in Fig. 2). Samples used in this study consisted of a total of 12 water samples (mixture of mine water—also called *fissure* water from underground at the ore deposits—used in cooling the drilling machine; waste water from the processing plant and 24 soil samples from each of the mine tailing dam, T1 & T2. It was observed that the slurry from the plant is deposited on the tailing dam in paddocks whose boundary contours are the edges of the different colors of the slurry, although some cross mixing can be seen. Figure 2 shows an example of a tailing with paddocks at different drying stages. These paddocks are filled from the outside inward and in a

Fig. 1 Water sampling points in the Carletonville goldfields Area of South Africa. From the top of this Fig.: DSW39/17-Water from DSW36/15 and DSW38/16; DSW36/15-Water from DSW9/14 and DSW42/10); DSW38/16-Discharge water from another mine; DSW42/10-Fissure water straight from underground; DSW9/14-Water from the settling point; DSW7/12-Water coming from the mine shaft and from process plants; DAM3/13-Water after (downstream of) the settling point; DSW43/19-Purified water; DSW40/5 & DSW40/7-Raw water from return water dam; DSW18/3 & DSW112-Sewage water from mine shaft; DSW45/1-water from mine shaft; WV16, WV9, WV13, WV14, WV15 & WV3-Borehole water for public use from West village

Fig. 2 Soil (tailing, T1 & T2) sampling points in the Carletonville goldfields area of South Africa, LHS is T1 & RHS is T2

sequential manner following the perimeter of the Tailing dam. Hence they dry in that same sequence, each paddock taking as long as more than a month to be reusable again (of course this depend on the size of the dam). The soil and some water samples were collected from the top of the tailing and the discharge canals respectively to represent uranium that has come from the milling and processing stage of the fuel cycle. Fissure water samples were also collected from the mine shafts outlets to represents uranium from the ore body.

Soil sample preparation

Soil, samples were digested using a Multiwave 3000, Anton Paar microwave oven. About 1 g of each sample was weighed into a Microwave digester vial and then digested with the *aqua regia* acid (3 mL of 55% HNO_3, 9 mL of 32% HCl) and 2 mL of 2% H_2O_2—which enhances the oxidation properties of nitric acid [14]) following standard procedures. The aqua regia extraction is capable of complete recovery for Cd, Cu, Pb (our target element) and Zn [15]. That is, the microwave rotor was transferred to a microwave reactor system for 20–45 min. Then an aliquot (10 mL) of each sample was transferred into a volumetric flask and topped up with Ultra pur distilled water up to 100 mL. They were stored at 4 °C for another 24 h. The reagents used were of Suprapur analytical grade (by Merck Laboratory Supplies Pvt. Ltd). The EPA Method 3052 used in the sample digestion achieves total sample decomposition [14].

Water sample digestion protocol

A whole set of 5 mL each of the water samples were mixed with 5 mL of nitric acid and 1 mL of hydrochloric acid and then left to digest in the Multiwave 3000, Anton Paar microwave oven for 24 h. A 10 mL aliquot of each digested sample was then transferred into volumetric flasks and topped up with Millipore Milli-Q system (resistivity 18 MΩ cm^{-1}) distilled water up to 100 mL and left overnight for ICP-MS analysis.

All digested sampled were then preserved at 4 °C for before analysis in the Laboratory [16].

Instrumentation

The Perkin Elmer, NeXION 300Q, Inductively Coupled Plasma Mass Spectrometer (ICP-MS), was used for all sample analysis in this work. It has a Quadrupole ion deflector that focuses the ion beam to the Dual mode detector. The Isotope-ratio precision of this instrument is defined for the isotope ratio of $^{107}Ag/^{109}Ag$ internal standard using a 25 µg/L solution, which is achieved by single-

point peak hopping with a relative standard deviation (= 100 × SD/AVERAGE, ((0)) of < 0.2% RSD [17]. The optimized operating parameters are summarized in Table 1.

Interference reduction

In the ICP-MS analysis of samples, the following molecular ions are potential sources of interferences; oxides, hydrides, hydroxides, nitrides [20–22]. Their effect can however be reduced by using the Perkin Elmer NexION 300Q's desolvating nebulizer. Also, the Instrument's Quadrupole ion deflector focuses only the selected isotopes in the ion beam, to the Dual mode detector. The other (interfering) ions are allowed to pass through to the waste [18, 23, 24]. Although the spectral resolution (0.7 amu) for this instrument is inadequate for discrete measurement of elements prone to sample-based spectral interferences, its collision-reaction cell technology render this problem as minor for the trace element determined in this work [25]. This capability of the NexION 300Q, combined with its Universal Cell Technology™, enables significant reduction in most or all the molecular ions in the sample [26, 27]. Also instrument drift is automatically corrected by the Software [28].

Sample run

The samples were loaded on to the auto sampler and initialized using the ICP-MS Instrument Control (Data Acquisition) Software. The instrument was set to Isotopic Ratio Method, operated in the Collision Mode for mass energy discrimination and filtration against interferences [24].

ICP-MS trace calibration for trace element analysis

For analysis of trace elements, the Perkin Elmer, NexION 300Q, (ICP-MS), calibration uses a Dual Detector Calibration Solution as the Atomic Spectrometric Standard, whose specifications are that:

In the Total Quantitative method, the mass calibration stability is measured using a 10 µg/L multi-element standards solution Al, Ba, Ce, Co, Cu, In, Li, Mg, Mn, Ni, Pb, Tb, U and Zn [17]. For every measurement, the Instrument was set to run a blank and a standard check at every ten samples for quality control.

Pb isotopic ratios data for geological CRMs

We have compared our results with those from USGS Reference materials as given in Schudel et al. [28] and the GeoMed Database [29], and Weis et al. [30].

Results and discussion

The results presented here are divided into two categories, *viz*; soil tailing and water samples. Due to lack of Certified Reference Materials to use in calibration check, the results presented here are approximated.

Table 1 NexION 300q ICP-MS instrumental parameters [18, 19]

Parameter	Value
Nebulizer	Glass concentric
Cones (sampler, skimmer, super-skimmer)	Nickel
Spray chamber	Glass cyclonic
Sample uptake rate	300 µL/min
Plasma gas flow	18.0 L/min
Auxiliary gas flow	1.2 L/min
Nebulizer gas flow	0.98 L/min (optimized for 2% CeO/Ce)
RF power	1600 W
Cell gas	Argon
Detector type value	Dual mode
Sweeps/reading	200
Readings/replicate	10
Replicates per sample	2
Mode/Universal Cell Technology™	Isotope ratio/collision mode
Internal standard	$^{107}Ag/^{109}Ag$ using a 25 µg/L solution
Total integration time	3.4 s

Soil tailing samples

The provenance of the Uranium, lead and other trace elements in the soil samples taken from tailing dam 1 and 2 are shown in Table 2.

Tables 3 and 4, shows the Pb–Pb and U–U isotopic ratios (respectively) for the Tailing soil samples. It can be concluded that there is good agreement between the sample ratios and the ULTRASPEC standard used to calibrate the Instrument. We note here that these results were acquired using an Agilent 7500 Series ICP-MS, in which the Multi-element calibration standards (from ULTRASPEC, SOUTH AFRICA), were used to validate the method. It is also noted that the results of the ULTRASPEC STD ratios are in god agreement with those found in the NIST data base. The authors could not use a NIST isotopic standard due to limitation of resources. However the ULTRASPEC standard contained U and Pb elements. This was assumed sufficient for identifying lead and uranium isotopic signatures.

Mine water results

Table 5 shows the atom percent abundances of the U and Pb in the water samples analyzed.

Table 2 Provenance of the uranium, lead and other trace elements in the soil samples taken from tailing dam 1 and 2 (ppm), with an average of $n = 3$ replications for each entry

Sample ID	Pb	Ba	K	Mg	Mn	Na	P	Sr	Th	U	Ni	Ti	Co	Mo	Li
T1E1	0.129	0.070	67.8	271	11.8	5.8	1.5	0.18	0.044	0.68	1.2	1.2	0.32	0.021	0.105
T1E2	0.076	0.022	53.9	201	10.1	4.3	2.2	0.10	0.044	0.62	0.9	1.1	0.28	0.016	0.058
T1E3	0.072	0.049	86.3	245	11.5	3.7	2.6	0.16	0.038	0.60	1.1	2.1	0.33	0.026	0.091
T1E4	0.076	0.046	94.5	273	11.4	7.9	2.9	0.16	0.042	0.72	1.4	1.5	0.49	0.020	0.101
T1E5	0.053	0.080	94.9	353	13.9	5.1	1.7	0.20	0.043	0.46	1.1	2.9	0.26	0.019	0.127
T1E6	0.089	0.032	22.8	117	5.9	2.5	0.6	0.10	0.040	0.04	0.8	0.3	0.23	0.011	0.043
T1E7	0.096	0.056	48.5	204	9.1	3.4	1.0	0.13	0.039	0.23	1.1	1.6	0.36	0.018	0.078
T1E8	0.071	0.038	37.4	165	8.1	4.2	1.0	0.12	0.042	0.00	1.0	0.4	0.34	0.022	0.069
T1E9	0.131	0.068	71.3	231	9.7	12.0	1.1	0.17	0.055	0.94	5.0	0.4	0.28	0.026	0.092
T1E10	0.105	0.057	38.9	195	11.2	2.2	0.9	0.13	0.088	1.37	1.8	0.5	0.57	0.013	0.075
T1E11	0.086	0.027	56.7	553	23.2	6.2	1.7	0.28	0.048	0.23	2.2	0.5	0.41	0.011	0.143
AVRG	0.090	0.050	61.2	255	11.4	5.2	1.6	0.16	0.048	0.53	1.6	1.1	0.35	0.019	0.089
MAX	0.131	0.080	94.9	553	23.2	12.0	2.9	0.28	0.088	1.37	5.0	2.9	0.57	0.026	0.143
MIN	0.053	0.022	22.8	117	5.9	2.2	0.6	0.10	0.038	0.00	0.8	0.3	0.23	0.011	0.043
SD	0.024	0.019	24.1	117	4.4	2.8	0.7	0.05	0.014	0.41	1.2	0.8	0.10	0.005	0.029
T2E1	0.068	0.034	27.3	292	8.4	6.3	1.3	0.14	0.030	0.54	3.2	0.4	0.18	0.012	0.053
T2E2	0.175	0.092	38.3	267	8.8	5.8	1.4	0.18	0.038	0.50	0.7	0.6	0.21	0.012	0.049
T2E3	0.172	0.160	183	1210	25.8	27.9	4.1	0.35	0.051	0.46	1.8	3.3	0.45	0.036	0.259
T2E4	0.159	0.069	93.2	854	19.9	8.6	2.7	0.20	0.064	0.68	2.4	1.8	5.19	0.058	0.162
T2E5	0.052	0.026	37.7	450	10.8	5.7	1.0	0.11	0.049	0.46	0.9	0.2	0.23	0.012	0.087
T2E6	0.041	0.030	33.6	388	9.4	4.6	1.0	0.09	0.050	0.68	0.9	0.2	0.25	0.014	0.080
T2E7	0.069	0.058	69.6	351	7.3	9.5	1.0	0.13	0.043	0.69	0.9	1.0	0.25	0.015	0.063
T2E8	0.087	0.125	152	810	15.8	9.3	2.1	0.25	0.059	0.83	1.5	2.5	0.33	0.026	0.138
T2E9	0.077	0.036	48.2	403	10.1	12.5	0.9	0.12	0.039	0.00	0.8	0.1	0.20	0.011	0.076
T2E10	0.100	0.088	114	685	14.5	14.9	1.5	0.20	0.058	0.61	1.2	1.2	0.31	0.012	0.135
T2E11	0.075	0.047	41.8	330	8.1	6.2	1.0	0.15	0.043	0.70	0.8	0.2	0.24	0.016	0.066
T2E12	0.281	0.060	68.5	305	4.6	4.5	0.9	0.09	0.044	0.23	1.0	0.5	0.48	0.019	0.055
T2E13	0.086	0.027	32.2	690	14.4	4.9	1.8	0.22	0.045	0.84	1.9	0.5	0.41	0.017	0.086
AVRG	0.111	0.066	72.3	541	12.1	9.3	1.6	0.17	0.047	0.55	1.4	1.0	0.67	0.020	0.101
MAX	0.281	0.160	183	1210	25.8	27.9	4.1	0.35	0.064	0.84	3.2	3.3	5.19	0.058	0.259
MIN	0.041	0.026	27.3	267	4.6	4.5	0.9	0.09	0.030	0.00	0.7	0.1	0.18	0.011	0.049
SD	0.068	0.041	49.9	287	5.8	6.4	0.9	0.07	0.009	0.24	0.8	1.0	1.36	0.013	0.060

Table 3 Pb-Pb isotopic ratios for tailings soil samples

Sample ID	Measured $^{207}Pb/^{206}Pb$	$^{208}Pb/^{206}Pb$ normalized $^{207}Pb/^{206}Pb$	Measured $^{208}Pb/^{206}Pb$	$^{208}Pb/^{206}Pb$ normalized $^{208}Pb/^{206}Pb$	Measured $^{204}Pb/^{206}Pb$	$^{208}Pb/^{206}Pb$ normalized $^{204}Pb/^{206}Pb$
T5W12	0.778 ± 0.053	0.832 ± 0.064	1.324 ± 0.072	1.646 ± 0.087	0.046 ± 0.004	0.057 ± 0.004
T5W15	0.678 ± 0.042	0.741 ± 0.073	1.026 ± 0.086	1430 ± 0.097	0.034 ± 0.003	0.036 ± 0.003
T5W8	0.996 ± 0.061	1.033 ± 0.067	1.936 ± 0.088	2.034 ± 0.073	0.060 ± 0.004	0.062 ± 0.003
T5W6	1.000 ± 0.033	1.042 ± 0.078	1.996 ± 0.062	2.069 ± 0.085	0.062 ± 0.003	0.060 ± 0.005
T5W5	1.162 ± 0.043	1.228 ± 0.058	2.380 ± 0.086	2.286 ± 0.052	0.074 ± 0.003	0.092 ± 0.002
T2E10	0.782 ± 0.042	0.815 ± 0.046	1.324 ± 0.074	1.656 ± 0.059	0.038 ± 0.004	0.048 ± 0.004
T2E11	0.760 ± 0.042	0.786 ± 0.045	1.262 ± 0.067	1.603 ± 0.056	0.024 ± 0.004	0.030 ± 0.005
T1E9	0.756 ± 0.057	0.780 ± 0.031	1.308 ± 0.057	1.635 ± 0.044	0.038 ± 0.045	0.048 ± 0.004
T1E8	0.754 ± 0.059	0.819 ± 0.037	1.280 ± 0.061	1.615 ± 0.084	0.038 ± 0.006	0.048 ± 0.005
T1E6	0.692 ± 0.031	0.718 ± 0.038	1.098 ± 0.057	1.485 ± 0.076	0.032 ± 0.004	0.043 ± 0.004
ULTRA SPEC STD		0.919 ± 0.078		2.171 ± 0.078		0.059 ± 0.004
NIST SRM 981 [31]		0.91464 ± 0.00033		2.1681 ± 0.0008		0.05904 ± 0.00004

Table 4 U-U isotopic ratios for tailing soil

Sample ID	Measured (×1E−5) $^{234}U/^{238}U$	Measured (×1E−3) $^{235}U/^{238}U$	Measured (×1E−3) $^{234}U/^{235}U$
TSW12	5.049 ± 0.038	8.546 ± 0.073	5.908 ± 0.004
TSW15	4.019 ± 0.041	8.883 ± 0.088	4.524 ± 0.003
TSW8	4.350 ± 0.036	8.847 ± 0.076	4.917 ± 0.004
TSW6	2.842 ± 0.059	8.849 ± 0.062	3.212 ± 0.003
TSW5	3.750 ± 0.029	8.721 ± 0.086	4.300 ± 0.003
T2E10	3.667 ± 0.034	6.688 ± 0.074	4.135 ± 0.004
T2E11	4.162 ± 0.074	8.894 ± 0.067	4.680 ± 0.004
T1E9	4.067 ± 0.042	8.962 ± 0.058	4.538 ± 0.045
T1E8	4.410 ± 0.069	8.942 ± 0.071	4.932 ± 0.006
T1E6	3.750 ± 0.031	8.885 ± 0.087	4.221 ± 0.004
ULTRASPEC STD (this work)	7.637 ± 0.025	7.385 ± 0.079	10.340 ± 0.004
DOE CRM 129-A [32]	5.3350 ± 0.0039	7.2614 ± 0.0039	7.3470 ± 0.0039

The results in Table 5 shows exceptionally high average abundance values of ^{235}U, for samples WV13, WV15, DSW7/12, much above natural uranium isotopic concentrations, probably due to anthropogenic processes. However the water samples are enhanced in ^{206}Pb which is a signature for a radiogenic ore deposit, as also evidenced by the normal Crustal levels for ^{204}Pb. Although sample WV13 is borehole water, the results show that this rock bed is highly depleted in ^{238}U. That would affect all the water samples from WV9, WV14 & WV15 as they are in the same area. There could be pyritic (sulphur containing) [34], hydrothermal underground water infiltration into the borehole waters and thus dissolving and leaching the uranium ore [7]. The bottom table shows a comparison with the NIST and US-DOE standard values for Pb and U respectively, and there is a good agreement.

The results from Table 6, show that all the DWS water samples from this mine have lead isotopic ratios close to the NIST SRM 981 values. These samples contain natural uranium from underground. This table also reveals the following characteristics of the mine. For the purified water (WVs) samples, the isotopic concentrations of the Pb isotopes varied widely from one sample to the other. However most of the samples from *fissure* water had close isotopic ratios. The concentration of ^{235}U in the *fissure* water shows that this sample is natural uranium before extraction by chemical processes, while that from the tailing has very low ^{235}U. This in itself is a signature that distinguishes

Table 5 Abundances of U and Pb in mine water samples (wt%)

Sample ID	^{238}U	^{235}U	^{234}U	^{204}Pb	^{206}Pb	^{207}Pb	^{208}Pb
WV15	98.00	1.88	0.12	1.27	26.26	21.30	51.17
WV14	99.13	0.83	0.03	1.43	26.37	21.80	50.37
DAM3/13	99.23	0.73	0.00	1.50	27.80	20.87	49.87
WV13	95.97	3.40	0.60	1.57	26.33	20.80	51.37
DSW9/14	99.27	0.70	0.00	1.07	29.00	21.10	48.83
DSW45/1	99.37	0.67	ND	1.16	31.65	20.88	46.32
DSW40/7	99.97	0.04	0.00	1.24	31.58	19.57	47.61
DSW7/12	98.63	1.03	0.33	1.43	25.70	22.10	50.73
DSW43/19	99.27	0.70	0.03	1.33	25.93	21.50	51.17
DSW39/17	98.93	0.87	0.27	1.33	25.90	20.83	51.97
DSW18/3	99.30	0.70	0.00	1.43	25.63	21.20	51.80
DSW40/5	99.17	0.83	0.00	1.47	25.77	21.37	51.37
AVER	98.85	1.03	0.13	1.35	27.33	21.11	50.21
SD	1.02	0.85	0.20	0.15	2.23	0.63	1.77
NIST SRM981 [31]				1.4255	24.1442	22.0833	52.3470
SD				0.0012	0.0057	0.0027	0.0086
US, DOE [33]	99.2746	0.72017	0.052458				
± SD	0.00039	0.00039	0.000008				

Table 6 Lead isotopic ratios for water samples before and after $^{208}Pb/^{206}Pb$ normalization for mass balance

Sample ID	Measured $^{207}Pb/^{206}Pb$	$^{208}Pb/^{206}Pb$ - normalized $^{207}Pb/^{206}Pb$	Measured $^{208}Pb/^{206}Pb$	$^{208}Pb/^{206}Pb$ normalized $^{208}Pb/^{206}Pb$	Measured $^{204}Pb/^{206}Pb$	$^{208}Pb/^{206}Pb$ normalized $^{204}Pb/^{206}Pb$
CW4	0.7715 ± 0.0531	0.8254 ± 0.0640	1.8575 ± 0.0972	1.987 ± 0.0873	0.0541 ± 0.0043	0.0578 ± 0.0037
WV14	0.8268 ± 0.0672	0.8738 ± 0.0734	1.9102 ± 0.0891	2.0187 ± 0.0978	0.0544 ± 0.0033	0.0574 ± 0.0025
DAM31/3	0.7506 ± 0.0691	0.8154 ± 0.0673	1.7938 ± 0.0876	1.9487 ± 0.0732	0.0540 ± 0.0041	0.0586 ± 0.0037
WV13	0.7899 ± 0.0593	0.8271 ± 0.0782	1.9506 ± 0.0962	2.0426 ± 0.0895	0.0595 ± 0.0036	0.0623 ± 0.0047
DSW9/14	0.7276 ± 0.0473	0.8128 ± 0.0687	1.6839 ± 0.0896	1.8810 ± 0.0852	0.0368 ± 0.0025	0.0411 ± 0.0023
DSW21/11	0.7488 ± 0.0642	0.8187 ± 0.0675	1.7678 ± 0.0794	1.9329 ± 0.0789	0.0451 ± 0.0036	0.0493 ± 0.0038
DSW199	0.8155 ± 0.0742	0.8454 ± 0.0674	1.9961 ± 0.0687	2.0693 ± 0.0796	0.0581 ± 0.0041	0.0602 ± 0.0046
DSW7/12	0.8599 ± 0.0657	0.8958 ± 0.0596	1.9741 ± 0.0587	2.0564 ± 0.0864	0.0558 ± 0.0453	0.0581 ± 0.0039
DSW43/19	0.8290 ± 0.0659	0.8638 ± 0.0769	1.9730 ± 0.0971	2.0558 ± 0.0897	0.0514 ± 0.0055	0.0536 ± 0.0047
DSW39/17	0.8044 ± 0.0731	0.8320 ± 0.0694	2.0064 ± 0.0897	2.0753 ± 0.0786	0.0515 ± 0.0043	0.0532 ± 0.0037
DSW18/3	0.8270 ± 0.0698	0.8528 ± 0.0654	2.0208 ± 0.0789	2.0837 ± 0.0698	0.0559 ± 0.0043	0.0577 ± 0.0051
DSW4/5	0.8292 ± 0.0711	0.8601 ± 0.0684	1.9935 ± 0.0848	2.0678 ± 0.0944	0.0569 ± 0.0041	0.0590 ± 0.0034
AVER	0.7984 ± 0.0685	0.8436 ± 0.0598	1.9107 ± 0.0786	2.0183 ± 0.0897	0.0528 ± 0.0046	0.0557 ± 0.0051
SD	0.0407	0.0261	0.1101	0.0660	0.0063	0.0058
%RSD	5.0929	3.0962	5.7614	3.2722	11.8801	10.3423
NIST SRM 981 [31]		0.91464± 0.00033		2.1681 ± 0.0008		0.059042 ± 0.000037

The standard error for the measurements of the ratios were ranging from $0.5 \leq \%RSD \leq 3$

between ore uranium and processed uranium for the South African mine investigated. For this mine too, the concentration of ^{206}Pb is unexpectedly high signifying ore deposits rich in ^{238}U.

For this geochronological study we use the fingerprint of the two ratios, $^{207}Pb/^{206}Pb$ and $^{208}Pb/^{206}Pb$ [11, 26]. The instrument mass bias corrected isotopic ratios of lead normalized to $^{208}Pb/^{206}Pb$ [35] are shown in Table 7 below. The advantage of using ^{206}Pb as the denominator isotope is that there is significantly less error magnification and much less error correlation between the measured ratios than for ratios to ^{204}Pb [35].

Table 7 Water sample results relative to ^{204}Pb for the mine area [36]

Sample ID	$^{208}Pb/^{204}Pb$	$^{207}Pb/^{204}Pb$	$^{206}Pb/^{204}Pb$
CW4	34.36	14.27	17.29
WV1/4	35.14	15.21	17.41
WV1/3	32.79	13.28	16.05
DAM3/13	33.24	13.91	17.06
DSW9/14	45.78	19.78	24.34
DSW21/11	39.17	16.59	20.27
DSW19/9	34.38	14.04	16.61
DSW7/12	35.40	15.42	17.21
DSW43/19	38.38	16.13	18.67
DSW39/17	38.98	15.63	18.78
DSW18/3	36.14	14.79	17.34
DSW45/1	35.02	14.57	16.94
AVER	36.56	15.30	18.16
SD	3.59	1.71	2.25
NIST SMR 981 [31]	36.72185 ± 0.0008	15.49161698 ± 0.00033	16.93736 ± 0.000037

The standard error for the measurements of the ratios were ranging from $0.5 \leq \%RSD \leq 3$

Table 7, shows that the uranium ore from which the sample mineralisation was found is a pyrite, with Pb ratios similar to that found by Jopoul et al. [36]. These results also show that the isotopic signatures are less radiogenic ($^{206}Pb/^{204}Pb \leq 20$). Also the Pb-Pb plot for these results (see our Fig. 3), confirm that the Carletonville gold fields are pyrite deposits, giving another signature for this mine. The similarity of these plots (data ranges) with those from Ref [36], suggest that the pyrites deposits are of detrital type.

The results of this work are relatively comparable with those from inter-laboratory comparisons although it is worthy pointing out that in those results [35], rigorous sample preparation and isotopic ratio corrections were effected than is done in this work.

In Fig. 3, lead (Pb) isotope ratios for this SA gold mine have $^{207}Pb/^{204}Pb$ values *distinctively ranging from about 13–20* and the $^{206}Pb/^{204}Pb$ values *are ranging from about 16–25*. This is distinctively different from lead samples in UK, Germany, Poland, Italy, and Spain [9]. According to Belluci et al., a $^{206}Pb/^{204}Pb$ ratio greater than 20 indicates that Pb investigated emanates from a uranium ore whereas a less ratio indicates a Pb-rich ore [37]. The U-bearing phases associated with the higher radiogenic Pb content are zircon, monazite and apatite [37]. This study had an extreme Pb $^{206}Pb/^{204}Pb$ ratio of *16–25* and it differs from

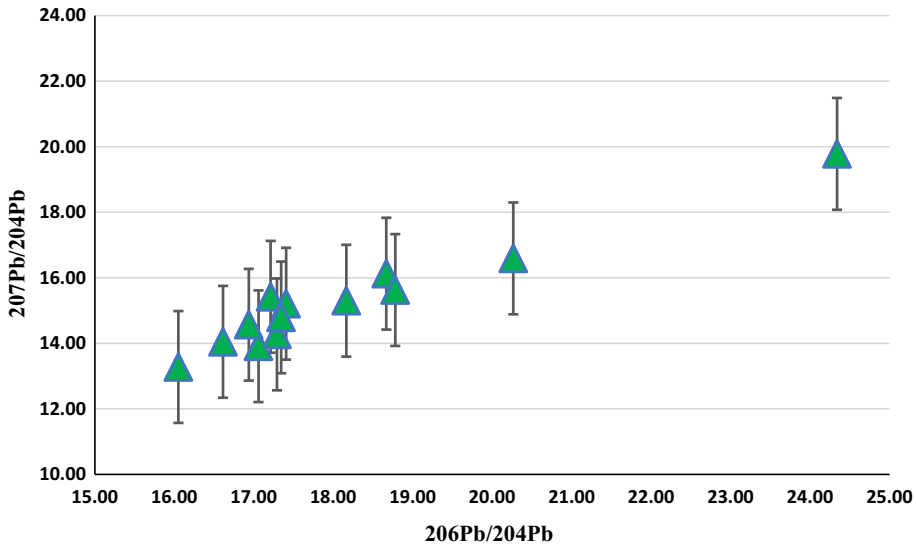

Fig. 3 A plot $^{207}Pb/^{204}Pb$ versus $^{206}Pb/^{204}Pb$ for mine (fissure) water samples

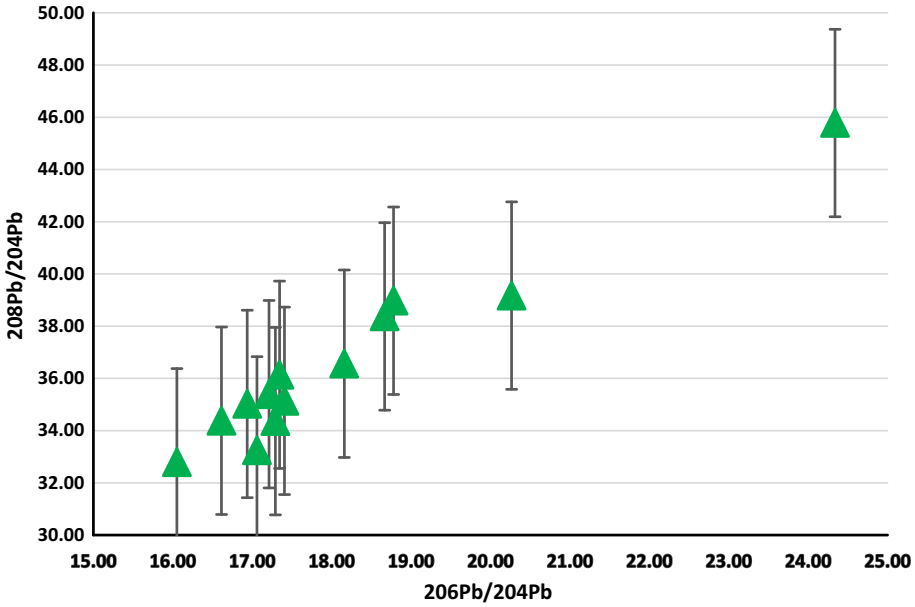

Fig. 4 A plot of $^{208}Pb/^{204}Pb$ versus $^{206}Pb/^{204}Pb$ for water samples

that of 17.6–18.0 in Belluci et al., studies which represent a Pb-ore Bunchas mine located in Newfoundland, Canada. As a result it can be used for as a signature for the mine examined in this study conducted here compared to the mine in Canada. The results of Fig. 3 further indicate that this signature from the tailing is more defined (reliable) with less scatter of the data. This could be because in the study area, each tailing dam receives only processing wastes from a particular selected mine shaft(s) which presumably extract from the same uranium ore zone underground. Also the mine (fissure) water from all shafts is pumped to the same discharge pipe where the researchers collected the fissure water at various points in the discharge. The ratios are all within expected ranges [9, 38].

Comparing Figs. 3 and 4, it is evidence that the signature for uranium in the mine (fissure) water, which contains uranium from the ore, is distinctly different in that the last two points in Figs. 3 and 4 are seemingly outliers (DSW9/14-water from the settling point, where all shaft mine waste deposits accumulates). A close look at the isotopes indicate that these two points are actually due to the observed much higher value of ^{206}Pb (implying higher ^{238}U concentration) and even lower value of ^{204}Pb (that is, these two deposits are of radiogenic origin [38]). Results in Fig. 4 indicate the geological origin of the deposit (radiogenic in this case). Here the $^{208}Pb/^{204}Pb$ values are *distinctively ranging from about 32–46.*

The characteristic signature of the lead isotope ratios from this mine can be seen in Fig. 5 where most of the data is scattered around $^{208}Pb/^{206}Pb = 2.05$ slightly less than the NIST SMR value of 2.07 probably due to lead loss in the ore. In Fig. 6 the data scatter around values of $^{204}Pb/^{206}Pb$

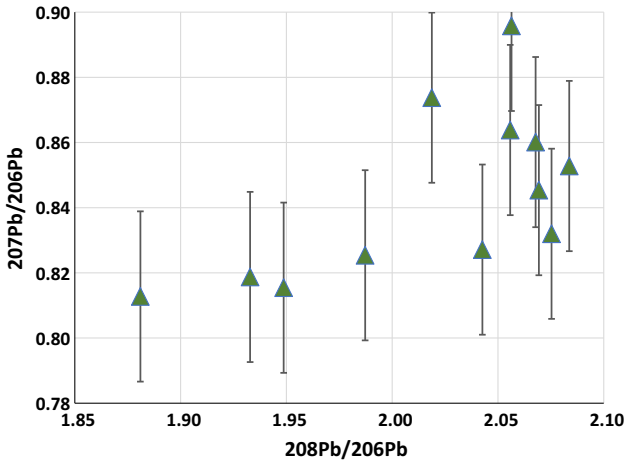

Fig. 5 $^{207}Pb/^{206}Pb$ versus $^{208}Pb/^{206}Pb$ for mine (fissure) water samples

= 0.059, which is in good agreement with the NIST SRM 981 [31] value of 0.59042.

Discussions

The NexION 300Q ICP-MS has a sensitivity > 40 mg/L and > 20 mg/L (for ^{24}Mg) with a detection limit of < 0.2 ng/L (for ^{238}U) [17]. The instrument Short-term precision is defined as the relative standard deviation (% RSD) for a 1 µg/L multi-element solution, measuring ^{24}Mg, ^{63}Cu, $1^{14}Cd$ and ^{208}Pb, without internal standardization. It is evaluated as < 3% RSD. It has an isotope-ratio precision which is defined for the isotope ratio of $^{107}Ag/^{109}Ag$ using

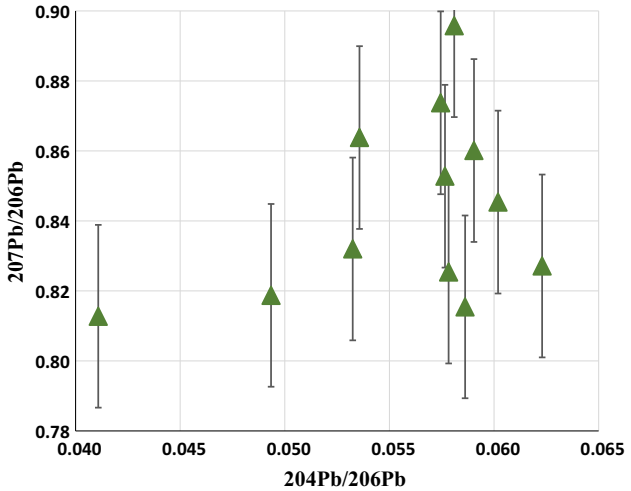

Fig. 6 Isotopic composition of the mine water samples relative to ^{206}Pb

a 25 µg/L solution. Obtained using single-point peak hopping this value is < 0.2% RSD.

The excellent sensitivity, precision and good accuracy of the ICP-MS operated under collision cell interface, has made it comparable to thermal ionization mass spectrometry (TIMS), for precise isotope ratio measurements. The ICP-MS configuration now allows for the dissociation, thermalizing and neutralizing of the disturbing argon-based molecular ions. The application of the collision cell in ICP-QMS results in a higher ion transmission, improved sensitivity and better precision of isotope ratio [39]. These characteristics formed the basis for using our Perkin Elmer NexION 300Q ICP-MS in this work.

TIMS results shown in Fig. 5b of Weis et al. [30], fall within the range shown in Figs. 3 and 4 of this work.

Sources of uncertainties

The Pb–Pb ratios in these results are relatively lower than the true values. This could imply that instrument optimization alone is not sufficient to correct for mass fractionation although the NexION ICP-MS instrument used here does not use laser ablation (the most common source of mass fractionation [26, 35].

In this work the uncertainties were evaluated as follows:

- For trace elements—uncertainties are presented as STDEV of all the results in the Tables.
- For Isotopic ratios—all results are average values of three replications by the instrument.
- For all graphs—we calculated the STDEV (σ) for each data set plotted and used that to plot the error bars as (± σ) for each point on the graph.

Lead isotopic signatures

The lead isotopes in mineral ores originate either from natural lead or radiogenic lead [40]. In this work, the isotopic composition of lead in the mine ores of Carletonville Gold fields was studied using the ICP-MS isotopic ratio technique as a tool for nuclear forensic investigations. To characterize different materials from the mine shafts, we measured the trace elementary impurities also. The lead isotopic composition of water direct from the mine shaft varied largely from those from the borehole or purified water. Thus this can be applied as a parameter to distinguish ore bodies from different origins.

Trace elements

The concentrations of the trace elements (Pb, Ba, K, La, Mg, Mn, Na, P, Sr, Th and U) reported here indicated that the uranium deposit in this mine is contained in pyrite type ores [7]. The mean values for Pb ranged around 0.090 ± 0.053 to 0.111 ± 0.068 ppm for soil tailing 1 & 2 respectively while U had ranges from 0.534 ± 0.406 in tailing 1 and a mean value of 0.555 ± 0.237 ppm in tailing 2. These amounts then seep into the water systems and could pose a radiochemical and radiological danger to animals and people utilizing the water taken from beyond DSW39/17 in Fig. 1. The concentrations were very high compared to the SA Department of Water Affairs and Forestry (DWAF) values 10 ppb for Pb and 40.5 ppb for U. The trace elemental impurities, show that their concentration in the mine tailing is different from that in the mine water which further support signature of the lead isotope data.

Conclusions

In this work, elemental and lead isotopic ratio analyses of uranium mine ores samples, from the 3 operating mine shafts and three operating tailing dams in South Africa were carried out to determine the lead isotopic signatures to be developed for use in identifying the origin of South African uranium. We conducted elemental analyses of samples from the two tailing dams nearest to the mine shafts using the inductively coupled plasma mass spectrometry (ICP-MS). Lead isotope ratios were measured using ICP-MS isotopic ratio technique. The trace elements concentrations indicated that the uranium and lead had concentrations indicative (signatory) a uranium ore possibly embedded in phosphorite (pyrite) deposit in Apatite and fluorapatite minerals, and is recovered from phosphoric

acid leaching followed by lime precipitation to remove impurities and magnesia is used for precipitation of the uranium [41]. The Lead ratios are found to fall within the certified values or standard reference. Also the Pb–Pb plot for these results confirm that the Carletonville gold fields are pyrite deposits, suggest that the pyrites deposits are of uraninite detrital type giving another nuclear forensic signature for this mine.

This work has demonstrated the viability of the ICP-MS Isotopic Ratio method as a techniques for developing nuclear forensics signatures for a South African mine. The nuclear forensic graphs presented here provide enough evidence to confirm that uranium ore signatures are indicative of the geochemical origins of an interdicted sample while those for the processed uranium points to the geographical origin.

Ore (water) samples were shown to contain balanced isotopic ratios of ^{238}U, ^{235}U and ^{234}U, while tailing samples revealed a depletion of these ratios maybe due to efficient modern processing techniques.

There is however, a need to expand this work to at least ten more mines with a wider geographical area in South Africa and also to verify these results with other techniques like TIMS or XRF. These will be most importantly applied in the next stage of the research, from an analytical and metrological point of view.

The researchers therefore will continue this investigation with samples from other mines and then follow each stage of the fuel cycle unto the uranium waste samples (spent fuel from the South African reactors). It is hoped that in 10 years' time South Africa will have a reliable nuclear forensics library for attribution and prosecution.

Acknowledgements Authors would like to acknowledge the International Atomic Energy Agency (IAEA) for sponsoring this Project under CRP J2003, (IAEA Research Contract No: 18777). The proof reading done by Dr John D. AUXIER II of the Institute for Nuclear Security at the University of Tennessee, Knoxville, during Mathuthu's IAEA Fellowship visit there in 2016, (IAEA SAF15007). The Principal Investigator (Mathuthu) acknowledges the Faculty Research Committee (FRC) [Grant No. G N150941] for financial support to attend and present this work at the Hungary Conference in July 2016. We also acknowledge the assistance provided by Lebo Motsei, Johann Hendricks and Tseole Mpho on the isotopic ratio technique.

References

1. Molgaard JJ, Auxier JD II, Giminaro AV, Oldham CJ, Cook MT, Young SA, Hall HL (2015) Development of synthetic nuclear melt glass for forensic analysis. J Radioanal Nucl Chem 304:1293–1301. https://doi.org/10.1007/s10967-015-3941-8
2. Varga Z (2008) Application of laser ablation inductively coupled plasma mass spectrometry for the isotopic analysis of single uranium particles. Anal Chim Acta 625:1–7. https://doi.org/10.1016/j.aca.2008.07.012
3. Molgaard JJ, Auxier JD II, Giminaro AV, Oldham CJ, Cook MT, Young SA, Hall HL (2015) Development of synthetic nuclear melt glass for forensic analysis. J Radioanal Nucl Chem 304(3):1293–1301. https://doi.org/10.1007/s10967-015-3941-8
4. Hutcheon ID, Kristo MJ, Knight KB (2005) Nonproliferation nuclear forensics. Glenn Seaborg Institute, Lawrence Livermore National Laboratory, Livermore
5. Kristo MJ (2012) Chapter 21—nuclear forensics. In: L'Annunziata MF (ed) Handbook of radioactivity analysis, 3rd edn. Academic Press, Amsterdam, pp 1281–1304. http://dx.doi.org/10.1016/B978-0-12-384873-4.00021-9
6. Moody KJG, Patrick M, Htcheon ID (2015) Nuclear forensic analysis, 2nd edn. CRC Press (Taylor and Francis Group), London, New York
7. Fuchs S, Williams-Jones AE, Przybylowicz WJ (2016) The origin of the gold and uranium ores of the Black Reef Formation, Transvaal Supergroup, South Africa. Ore Geol Rev 72:149–164. https://doi.org/10.1016/j.oregeorev.2015.07.010
8. Varga Z, Katona R, Stefanka Z, Wallenius M, Mayer K, Nicholl A (2010) Determination of rare-earth elements in uranium bearing materails by binductively coupled plasma mass spectrometry. Talanta 80:1744–1749. https://doi.org/10.1016/j.talanta.2009.10.018
9. Balcaen L, Moens L, Vanhaecke F (2010) Determination of isotope ratios of metals (and metalloids) by means of inductively coupled plasma-mass spectrometry for provenancing purposes—a review. Spectrochimica Acta Part B 65:769–786. https://doi.org/10.1016/j.sab.2010.06.005
10. Andersen T (2002) Correction of common lead in U-Pb analyses that do not report 204Pb. Chem Geol 192:59–79
11. Cheng H, Hu Y (2010) Lead (Pb) isotopic fingerprinting and its applications in lead pollution studies in China: a review. Environ Pollut 158(158):1134–1146. https://doi.org/10.1016/j.envpol.2009.12.028
12. Balboni E, Nina J, Spano T, Simonetti A, Burns PC (2016) Chemical and Sr isotopic characterization of North America uranium ores: nuclear forensic applications. Appl Geochem 74:24–32. https://doi.org/10.1016/j.apgeochem.2016.08.016
13. SAHO (2016) Colonial history and development of Johannesburg. South African History Online 1
14. Mangum SJ (2009) ICP-optical emission spectrometry and ICP-mass spectrometry. Field Application Report, pp 1–3
15. Gaudino S, Galas C, Belli M, Barbizzi S, de Zorzi P, Jaćimović R, Jeran Z, Pati A, Sansone U (2007) The role of different soil sample digestion methods on trace elements analysis: a comparison of ICP-MS and INAA measurement results. Accred Qual Assur 12(2):84–93. https://doi.org/10.1007/s00769-006-0238-1
16. Kamunda C, Mathuthu M, Madhuku M (2016) Assessment of radiological hazards from gold mine tailings in Gauteng Province, South Africa. 016, 13(1), 138; http://dx.doi.org/. Int J Environ Res Public Health 13(1):138–148. 10.3390/ijerph13010138
17. PerkinElmer W (2010) NexION 300Q ICP-MS specifications ICP-MS Spectrometry. PerkinElmer, Inc, Waltham, pp 1–2
18. Bosnak C, Pruszkowski E (2014) The analysis of drinking waters by U.S. EPA method 200.8 using the NexION 300D/350D ICP-MS in standard, collision and reaction modes. PerkinElmer, IncShelton, CT application brief ICP-Mass Spectrometry, pp 1–4
19. CaEP Bosnak (2014) APPLICATION BRIEF ICP-Mass Spectrometry: The Elemental Analysis of Spinach with the NexION 300/350 ICP-MS. PerkinElmer, IncShelton, pp 1–4
20. Horn I, Rudnick RL, McDonough WF (2000) Precise elemental and isotope ratio determination by simultaneous solution nebulization and laser ablation-ICP-MS: application to U-Pb geochronology. Chem Geol 164(3–4):281–301. https://doi.org/10.1016/S0009-2541(99)00168-0

21. Thirlwall MF, Anczkiewicz R (2004) Multidynamic isotope ratio analysis using MC–ICP–MS and the causes of secular drift in Hf, Nd and Pb isotope ratios. Int J Mass Spectrom 235(1):59–81. https://doi.org/10.1016/j.ijms.2004.04.002
22. Verni ER, Londonio A, Bazána C, Strasser E, Perino E, Gil RA (2017) REE profiling in basic volcanic rocks after ultrasonic sample treatment and ICPMS analysis with oxide ion formation in ICP enriched with O2. Microchem J 130:14–20. https://doi.org/10.1016/j.microc.2016.07.014
23. Mangum S (2015) Uranium isotope ratio measurements with the NexION ICP-MS. Perkin Elmer Inc Shelton, CT application note: ICP-mass spectrometry, pp 1–4
24. Vilta M (2016) NexION 300 ICP-MS instruments animation. Perkin Elmer Inc. Shelton. https://www.youtube.com/watch?v=L-FYh2z9mi0. Accessed 15 November 2016
25. UT JSoG (2017) Quadrupole ICP-MS lab: teaching activities and resources. The University of Texas at Austin, pp 1–13
26. Lin J, Liu Y, Yang Y, Hu Z (2016) Calibration and correction of LA-ICP-MS and LA-MC-ICP-MS analyses for element contents and isotopic ratios. Solid Earth Sciences 1(1):5–27. https://doi.org/10.1016/j.sesci.2016.04.002
27. Woods G (2014) Lead isotope analysis: removal of 204Hg isobaric interference from 204Pb using ICP-QQQ in MS/MS mode: application note. Agilent Technologies, pp 1–8
28. Schudel G, Lai V, Gordon K, Weis D (2015) Trace element characterization of USGS reference materials by HR-ICP-MS and Q-ICP-MS. Chem Geol 410:223–236. https://doi.org/10.1016/j.chemgeo.2015.06.006
29. Jochum KP, Stoll B, Herwig K, Amini M, Abouchami W, Hofmann AW (2005) Lead isotope ratio measurements in geological glasses by laser ablation-sector field-ICP mass spectrometry (LA-SF-ICPMS). Int J Mass Spectrom 242(2–3):281–289. https://doi.org/10.1016/j.ijms.2004.11.019
30. Weis D, Kieffer B, Maerschalk C, Barling J, de Jong J, Williams GA, Hanano D, Pretorius W, Mattielli N, Scoates JS, Goolaerts A, Friedman RM, Mahoney JB (2006) High-precision isotopic characterization of USGS reference materials by TIMS and MC-ICP-MS. Geochem Geophys Geosyst (G3) 7(8):1–30. https://doi.org/10.1029/2006GC001283
31. Nist U (1991) Common Lead Isotopic Standard: Standard Reference Material 981 National Institute of Standrds and Technology. NIST, Gaithersburg, p 20899
32. Anl U (2008) Certificate of Analysis CRM 129-A Uranium Oxide (U3O8) Assay and Isotopic Standard. Deaprtment of Energy, Illinois, USA, USA
33. Energy USDo (2002) Uranium (normal) metal assay and isotopic standard. Certificate of Analysis CRM 112-A. New Brunswick Laboratory, ANL, Illinois
34. Barton ES, Hallbauer DK (1996) Trace-element and U-Pb isotope compositions of pyrite types in the Proterozoic Black Reef, Transvaal Sequence, South Africa: implications on genesis and ag. Chem Geol 133(133):173–199
35. Thirlwall MF (2000) Inter-laboratory and other errors in Pb isotope analyses investigated using a 207Pb–204Pb double spike. Chem Geol 163(1–4):299–322. https://doi.org/10.1016/S0009-2541(99)00135-7
36. Poujol M, Robbb LJ, Respauta JP (1999) U-Pb and Pb–Pb isotopic studies relating to the origin of gold mineralization in the Evander Goldfield, Witwatersrand Basin, South Africa. Precambr Res 95:167–185
37. Bellucci JJ, Simonetti A, Wallace C, Koeman EC, Burns PC (2013) Lead isotopic composition of trinitite melt glass: evidence for the presence of Canadian industrial lead in the first atomic weapon test. Anal Chem 85(15):7588–7593
38. Fahey AJ, Rictchie NWM, Newbury DE, Small JA (2010) The use of lead isotopiuc abundances in trace uranium samples for nuclear forensics analysis. J Radioann Nucl Chem 284:575–581. https://doi.org/10.1007/s10967-010-0509-5
39. Becker JS, Dietze HJ (2000) Precise and accurate isotope ratio measurements by ICP-MS. Fresen J Anal Chem 361(1):23–30. https://doi.org/10.1007/s002160000481
40. Švedkauskaite-LeGore J, Mayer K, Millet S, Baltrunas D (2007) Investigation of the isotopic composition of lead and of trace elements concentrations in natural uranium materials as a signature in nuclear forensics. Radiochim Acta 95(10):601–605. https://doi.org/10.1524/ract.2007.95.10.601
41. Keegan E, Richter S, Kelly I, Alonso-Munoz A (2008) The provenance of Australian U ore concentrates by elemental and isotopic analysis. Appl Geochem 23(4):765–777. https://doi.org/10.1016/j.apgeochem.2007.12.004